

Use of quantitative shotgun proteomics to identify fibronectin 1 as a potential plasma biomarker for clear cell carcinoma of the kidney

Akira Yokomizo^{a,*1}, Michiko Takakura^{b,1}, Yae Kanai^c, Tomohiro Sakuma^d, Junichi Matsubara^b, Kazufumi Honda^b, Seiji Naito^a, Tesshi Yamada^b and Masaya Ono^b

^aDepartment of Urology, Graduate School Medical Sciences, Kyushu University, Fukuoka, Japan

^bDivision of Chemotherapy and Clinical Research, National Cancer Center Research Institute, Tokyo, Japan

^cDivision of Molecular Pathology, National Cancer Center Research Institute, Tokyo, Japan

^dBioBusiness Group, Mitsui Knowledge Industry, Tokyo, Japan

Abstract. *Background:* Early detection would be one of the most effective means to improve the outcome of renal cell carcinoma (RCC). We searched for a new plasma marker for RCC using a label-free quantitative shotgun proteomics method.

Methods: Plasma proteins were digested by trypsin, and the resulting peptides were analyzed by 2-Dimensional Image Converted Analysis of Liquid chromatography mass spectrometry (2DICAL). An identified biomarker candidate was subjected to validation using the Amplified Luminescent Proximity Homogeneous Assay (AlphaLISA).

Results: Among a total of 23,407 independent MS peaks, we found that the mean intensity of 59 peaks significantly differed between 20 clear cell RCC patients and 20 healthy controls. MS/MS spectra from 16 of the 59 peaks matched the amino acid sequences of the fibronectin 1 (*FN1*) gene product. The increased plasma level of FN1 in RCC patients was validated in a cohort of 77 patients and 130 healthy controls ($p < 0.0001$).

Conclusions: The FN1 is considered to be a promising biomarker candidate for clear cell RCC. Furthermore, AlphaLISA is an alternate to the conventional enzyme-linked immunosorbent assay and should prove useful for the rapid validation of biomarker candidates.

Keywords: Renal cell carcinoma, tumor marker, proteomics, fibronectin

1. Introduction

The incidence of renal cell carcinoma (RCC) has been increasing since 1980s in western countries as well as Japan and is now the third most common malignancy of the urinary tract following prostate and bladder cancers [1]. Although early detection and treatment are considered to be the most effective methods to improve the outcome of patients with any cancer, RCC

patients often do not manifest clinical symptoms and receive medical attention until their tumors progress to advanced stages [2–4]. Recently, ultrasound and CT scan can detect smaller renal tumors. However, we do need an effective plasma biomarker for differentiating the malignant from the benign when a patient was found with a small renal mass, which cannot be easily judged from ultrasound or CT scan [5]. Therefore, it is necessary to identify the tumor marker better than neither ultrasound test nor CT scan in diagnosing small renal mass. If a sensitive but non-invasive blood assay that can detect early-stage RCC were available, it would greatly improve the curative rate of RCC.

Shotgun proteomics is an established technique in which whole proteins are enzymatically digested into a large array of small peptide fragments followed

*Corresponding author: Akira Yokomizo, Department of Urology, Graduate School of Medical Sciences, Kyushu University, 3-1-1 Maidashi, Higashi-ku, Fukuoka 812-8252, Japan. Tel.: +81 92 642 5603; Fax: +81 92 642 5618; E-mail: yokoa@uro.med.kyushu-u.ac.jp.

¹These two authors contributed equally to this work.

by direct analysis by liquid chromatography and mass spectrometry (LC-MS). We previously developed software named 2DICAL that can provide a quantitative dimension to shotgun proteomics [6]. 2DICAL can accurately align different LC-MS data and compare the protein content of a theoretically unlimited number of samples without isotope labeling [7]. 2DICAL is highly advantageous methods in clinical studies that require the comparison of a statistically sufficient number of patient samples [8]. Using 2DICAL, we were able to identify diagnostic biomarkers for endometrial and pancreatic cancers [7,8] and predictive biomarkers for hematologic toxicities and therapeutic efficacy of gemcitabine treatment to patients with advanced pancreatic cancer [9].

In this study we compared the plasma proteome between RCC patients and healthy controls using 2DICAL with the aim to identify a new diagnostic biomarker that can be used for a blood test. RCC consists of clear cell (75%), papillary (10%), chromophobe (5%) and other subtypes [10], and we first focused on clear cell carcinoma, the most common subtype of RCC. We discovered a significant increase of circulating plasma FN1 in patients with RCC and confirmed its significance in a larger patient cohort using a newly established measurement system.

2. Materials and methods

2.1. Plasma samples

Plasma samples were prospectively collected from RCC patients, prostate cancer patients and healthy volunteers at the Department of Urology, Kyushu University Hospital (Fukuoka, Japan) between October 2000 and January 2008. To exclude sampling bias, all the patients' whole blood (7 ml) was collected in the same tube (EDTA-2Na tube, Venocjet II, Terumo, Japan) before the surgery or first treatment. These blood samples were stored in 4°C for 1 hour and plasma was separated after centrifugation, aliquoted into 1 ml samples in 1.5 ml eppendorf tubes, and stored at -80°C. The control samples were collected and stored under the same condition. All the samples had the only one cycle of freeze-and-thaw. As we excluded the non-clear cell subtype and benign kidney tumors, the plasma from 77 histopathologically proven clear cell cancer patients were used for the analysis. Control plasma samples were randomly selected from 20 patients with prostate cancer and 130 healthy individuals after adjusting the

age and gender. The clinical stage of each patient was classified according to the 7th edition UICC TNM classification [11]. Twenty RCC patients (excluding those in stage IV) were selected for analysis using 2DICAL in an effort to detect early stage biomarkers (Table 1).

2.2. Ethics

All individuals provided written informed consent authorizing the collection and use of their samples for research purposes. The protocol was reviewed and approved by the institutional ethics committee boards of the National Cancer Center Research Institute (Tokyo, Japan) and the Kyushu University (Fukuoka, Japan).

2.3. LC-MS

The 20 most abundant plasma proteins including albumin and immunoglobulin were removed using Prot-Prep 20 Plasma Immunodepletion Kit (Sigma-Aldrich, St. Louis, MO) following the manufacturer's instructions. The depleted plasma samples were then digested with trypsin (Promega, Madison, WI) overnight at 37°C. The resulting peptides were randomized and measured in triplicate by LC-MS. LC separation in a linear gradient of 0 to 80% acetonitrile in 0.1% formic acid at a speed of 200 nL/minute for 60 minutes was conducted using a splitless nano-flow HPLC system (Hitachi High-technologies, Tokyo, Japan). MS data were acquired every second for 60 minutes by an electrospray ionization mass spectrometer (Q-TOF Ultima; Waters, Milford, MA) directly linked to an LC in the range of 250–1600 m/z. MS peaks were detected, normalized, and quantified using the in-house 2DICAL software package as described previously [7]. A serial ID number was applied to each of the MS peaks detected (ID 1 to 23,407) [9]. The stability of LC-MS was monitored by calculating the correlation coefficient (CC) and coefficient of variance (CV) values among triplicate measurements.

2.4. Protein identification by tandem mass spectrometry (MS/MS)

Peak lists were generated using the Mass Navigator software package (version 1.2) (Mitsui Knowledge Industry, Tokyo, Japan) and searched against the SwissProt database (SwissProt_57.6.fasta) using the Mascot software package (version 2.2.06) (Matrix Science, London, UK). The search parameters used were as follows: A database of human proteins was selected.

Table 1
Clinicopathological characteristics of individuals examined in this study

	(mean \pm SD)	Cases analyzed by AlphaLISA (n = 227)			Cases analyzed by 2DICAL (n = 60)	
		RCC (n = 77)	PCa (n = 20)	Healthy (n = 130)	RCC (n = 20)	Healthy (n = 20)
Age		61.2 \pm 11.0	64.8 \pm 6.9	65.4 \pm 10.5	63.8 \pm 8.5	66.0 \pm 7.9
Gender						
Male		57	20	113	20	20
Female		20		17	0	0
Clinical stage*						
I		56	9		17	
II		3	11		2	
III		3			1	
IV		9			0	
Unknown		6				
Tumor side						
Right		38			11	
Left		39			9	
Histologic type						
Clear cell		77			20	
Chromophobe		0			0	
Papillary		0			0	
Unclassified		0			0	

*according to TNM Classification of Malignant Tumors (International Union Against Cancer), 7th Edition

RCC, renal cell carcinoma; PCa, prostate cancer; AlphaLISA, amplified luminescence proximity homogeneous assay; 2DICAL, two-dimensional image convert

Trypsin was designated as the enzyme, and up to one missed cleavage was allowed. Mass tolerances for precursor and fragment ions were \pm 0.2 Da and \pm 0.8 Da, respectively. The score threshold was set to the value over 20 for peptide search. If a peptide matched to multiple proteins, the protein name with the highest Mascot score was selected.

2.5. Western blot analysis

Plasma samples were fractionated with SDS-PAGE and electroblotted onto a polyvinylidene difluoride membrane (Millipore, Billerica, MA), as described previously [9,12]. Primary antibodies used were mouse monoclonal anti-FN1 antibody (R&D Systems, Minneapolis, MN) and mouse monoclonal antibody against human complement C3b- α (PROGEN, Heidelberg, Germany) [8]. The membrane was then incubated with the primary antibody and subsequently with the relevant horseradish peroxidase-conjugated anti-mouse IgG as described previously. Blots were developed using an enhanced chemiluminescence (ECL plus) detection system (GE Healthcare, Buckinghamshire, UK).

2.6. AlphaLISA

An assay for measuring soluble FN1 was constructed using the AlphaLISA system (PerkinElmer, MA) which is a bead-bead nonradioactive technology. In brief, when a biological interaction brings the beads into close

proximity, a cascade of chemical reactions is induced resulting in a greatly amplified signal, then a photosensitizer present in the beads converts ambient oxygen to a more excited singlet state upon laser excitation. Biotinylated rabbit polyclonal anti-FN1 antibody and mouse polyclonal anti-FN1 antibody were purchased from Abcam (Cambridge, UK). The AlphaLISA procedure was carried out according to the protocol provided by the manufacturer.

2.7. Statistical methods

The Mann-Whitney U-test was employed for statistical analysis of the correlation between RCC patients and controls as well as the plasma values of FN1 and clinicopathological parameters. Welch's *t*-test was employed for 2DICAL analysis. Kaplan-Meier analysis was used to examine the correlation of the plasma value of FN1, cancer-specific survival and overall survival. The area under the curve (AUC) of the receiver operating characteristic (ROC) was calculated to evaluate its diagnostic significance.

3. Results

3.1. Identification of plasma proteins significantly increased in RCC patients

Plasma proteins of 20 patients with RCC and 20 healthy individuals were digested by trypsin, and

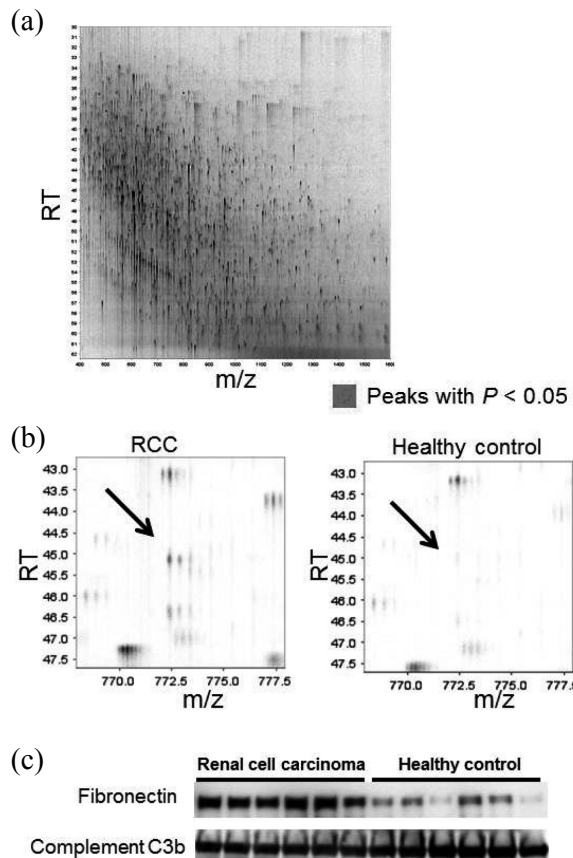


Fig. 1. (a) Two-dimensional display of all the MS peaks in 2DICAL. The 59 MS peaks whose mean intensity significantly differed in renal cell carcinoma patients from healthy controls ($p < 0.05$, Welch's t -test) are highlighted in red. (b) Two representative MS peaks with the smallest p -value. RT; retention time. (c) Detection of plasma FN1 and complement C3b- α (loading control) by immunoblotting.

the resulting peptides were subjected to LC-MS. A total of 23,407 MS peaks per sample were detected in the range of 250–1,600 m/z and 25–65 minutes across the 40 plasma samples, and their relative mass intensity was calculated using 2DICAL. The mean CC and CV values of the 23,407 MS peaks were over 0.95 and under 0.15, respectively, confirming the high reproducibility of LC-MS. Among the 23,407 MS peaks we found that the mean intensity of 59 peaks (in triplicate) significantly differed between 20 RCC patients and 20 healthy controls ($p < 0.05$, Welch's t -test). Thirty six peaks were increased and 23 peaks were decreased in RCC patients and the statistical significance was confirmed by calculating the false discovery rate (FDR) values [13] (data not shown). Figure 1a shows a representative 2-dimensional view in which all the $\sim 23,000$ MS peaks were displayed with the m/z along

the X axis and the RT of LC along the Y axis and the 59 MS peaks are highlighted in red. Figure 1b shows a representative MS peak that increased in the plasma of RCC patients.

3.2. Protein identification by MS/MS

Fifty seven MS/MS spectra acquired from the 59 MS peaks matched to 21 peptide sequences deposited in the human protein database (Table 2). Remarkably, 16 of the 21 peptides were found to be derived from the amino acid sequence of *FN1* gene product (Supportive information Figs S1 and S2). The identification and differential expression of FN1 protein were confirmed by immunoblotting (Fig. 1c).

3.3. Verification by AlphaLISA

To validate the increased level of plasma FN1, we constructed a new assay that can quantify the amount of FN1. The AlphaLISA showed high reproducibility with a median CV value of 0.08 among triplicates and linearity in the range of 50–800 $\mu\text{g}/\text{ml}$.

The plasma concentration of FN1 was measured in 77 RCC patients, 20 prostate cancer (PCa) patients, and 130 healthy individuals by AlphaLISA. There was a significant difference between RCC patients ($405 \pm 153 \mu\text{g}/\text{ml}$) and healthy individuals ($294 \pm 102 \mu\text{g}/\text{ml}$) with a p -value of 1.8×10^{-7} (Mann-Whitney U test) (Fig. 2a). The plasma concentration of FN1 was not elevated in PCa patients ($306 \pm 81 \mu\text{g}/\text{ml}$). The AUC value of ROC for plasma FN1 concentration of RCC patients to healthy individuals was calculated to be 0.71 for all stages, stage I and II and stage III and IV (Fig. 2b). The optimum diagnostic cut-off point of FN1 was identified at $377 \mu\text{g}/\text{ml}$ by the AUC curve. At this point, sensitivity, specificity, PPV and NPV were 53%, 82%, 64% and 75% respectively. And the fibronectin concentration in each clinical stage was shown in Fig. 2c.

3.4. Correlation of plasma concentration of FN1 and clinicopathological parameters

The statistical analyses were performed to detect the correlation of plasma concentration of FN1 and clinical stage (Fig. 2c), but there were no significant differences. Also, there were no significant correlations between concentration of FN1 and the other clinicopathological parameters, such as tumor size, tumor grade and vascular involvement (data not shown). Furthermore, Kaplan-Meier analysis, used to analyze the correlation

Table 2
Summary of protein identification by tandem mass spectrometry

ID	<i>m/z</i>	RT	Charge	Control (mean \pm SD)	RCC (mean \pm SD)	P Values **	Mascot Score	Peptide sequence	Protein description
2411	799.3815	36.479	3	15 \pm 6	25 \pm 13	5.09E-03	84.46	RPGGEPSPEGTTGGQSYNQYSQR	Fibronectin
3454	622.3328	39.679	3	14 \pm 4	20 \pm 8	8.59E-03	75.78	HTSVQTSSGSGPFTDVR	Fibronectin
3948	647.3662	49.283	2	13 \pm 2	17 \pm 7	9.54E-03	54.92	DLQFVEVTDVK	Fibronectin
2039	978.5337	47.716	2	16 \pm 7	30 \pm 20	6.08E-03	53.45	EESPLLIGQQSTVSDVPR	Fibronectin
750	706.3586	44.432	2	101 \pm 45	73 \pm 28	2.34E-02	51.41	KWQEEMELYR	Apolipoprotein A-I
2614	815.4614	46.26	2	11 \pm 4	18 \pm 12	1.61E-02	50.73	VDVIPVNLPGEHQR	Fibronectin
2068	646.379	52.817	2	17 \pm 7	26 \pm 15	1.96E-02	46.43	GATYNIIIVEALK	Fibronectin
2854	997.5346	53.967	2	18 \pm 5	23 \pm 11	4.61E-02	41.28	NTFAEVTLGLSPGVYYFK	Fibronectin
1231	675.3681	45.847	2	28 \pm 11	52 \pm 34	4.38E-03	40.93	WLPSSSPVTGYR	Fibronectin
1816	772.8941	45.207	2	17 \pm 7	32 \pm 20	5.88E-03	35.57	SYTITGLQPGTDYK	Fibronectin
2439	638.3344	38.15	2	22 \pm 7	30 \pm 13	1.54E-02	32.64	HVVPNENVVQR	Gelsolin
2569	555.8103	40.153	2	16 \pm 5	25 \pm 13	6.00E-03	32.26	STTPDITGYR	Fibronectin
1155	772.419	45.123	2	43 \pm 14	64 \pm 34	1.27E-02	31.79	SYTITGLQPGTDYK	Fibronectin
2771	701.8697	39.773	2	13 \pm 5	22 \pm 13	6.58E-03	30.7	HYQINQQWER	Fibronectin
2611	592.8548	43.895	2	26 \pm 11	19 \pm 6	1.87E-02	30.31	IQNLTTEEPK	Serum paraoxonase
1371	511.785	35.131	2	44 \pm 12	55 \pm 17	1.82E-02	29.99	ATVYVQGER	Beta-2-glycoprotein 1
1826	867.5129	50.364	2	20 \pm 7	36 \pm 22	3.48E-03	29.17	NLQPASEYTVSLVAIK	Fibronectin
1813	701.366	39.859	2	28 \pm 7	42 \pm 18	4.02E-03	27.25	HYQINQQWER	Fibronectin
2417	576.8117	42.453	2	16 \pm 5	26 \pm 15	5.75E-03	26.67	FTNIGPDTMR	Fibronectin
1794	964.0527	58.428	2	23 \pm 8	34 \pm 20	2.61E-02	23.59	VTWAPPSIDLTNFLVR	Fibronectin
1377	629.36	53.672	2	39 \pm 23	24 \pm 9	7.97E-03	21.25	DLAVVDAKDAIK	EXOC1_HUMAN

RT, retention time; RCC, renal cell carcinoma

**Welch's t-test.

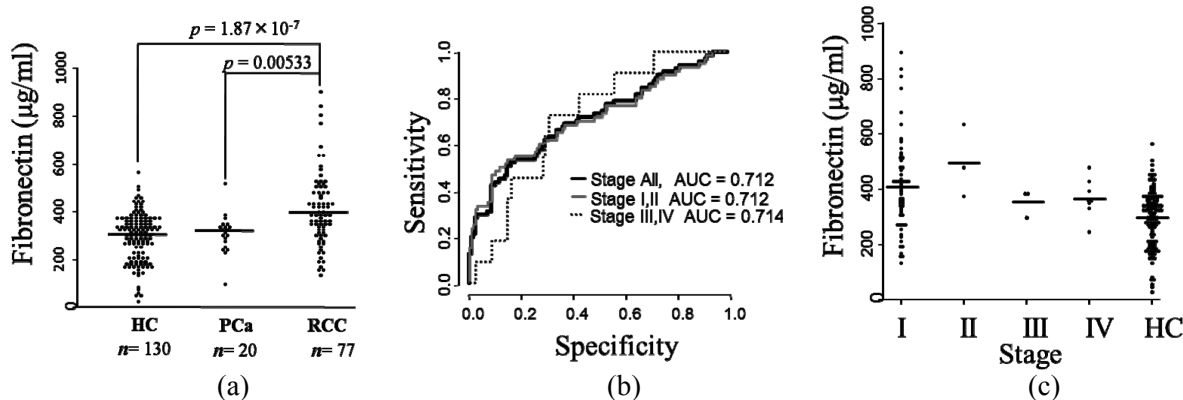


Fig. 2. (a) Concentration of plasma FN1 in each group. The FN1 concentration of renal cell carcinoma patients ($n = 77$), healthy individuals ($n = 130$) and prostate cancer patients ($n = 20$) was measured by AlphaLISA. There were significant differences in renal cell carcinoma patients compared to healthy individuals and prostate cancer patients, but not between healthy individuals and prostate cancer patients (Mann-Whitney U test). Horizontal lines represent the average concentration. (b) Receiver operating characteristic (ROC) curve for plasma FN1 concentration. AUC value of ROC for plasma FN1 concentration of RCC patients to healthy individuals was calculated to be 0.71 for all stages, stage I and II and stage III and IV. Similar AUC value of earlier stage to advanced stage suggested the possibility of early detection of renal cell carcinoma by plasma FN1. (c) The plasma FN1 concentration in each clinical stage. HC; healthy control.

of serum value of FN1, cancer-specific survival and overall survival, failed to prove any statistical significant differences with a median follow up of 47.6 months after surgery (data not shown).

4. Discussion

FN1 is a high-molecular-weight extracellular matrix protein that plays an important role in cellular at-

tachment and cell spread [14,15]. FN1 can be soluble or insoluble, is produced by hepatocytes and various cell types and is bound to integrins [16]. Altered expression of FN1 is known to change the morphology of several tumor cell lines [17]. In several studies of different RCC cell lines, FN1 was shown to be secreted into the culture medium and suggested to influence the movement and invasion of these cells [18–20]. Another study showed FN1 plasma levels signif-

icantly elevated in localized and metastatic RCC patients compared to a control group [21]. According to “THE HUMAN PROTEIN ATLAS” (<http://www.proteinatlas.org/ENSG00000115414>), FN1 is expressed in extracellular matrix and stromal cell. FN1 is expressed weakly in normal kidney and relatively higher expressed in kidney cancer. It could be considerable that higher plasma levels of FN1 is secreted from these extracellular matrix and stromal cell in kidney cancer. A recent study suggested that FN1 mRNA expression was higher in RCC compared to normal renal tissue and correlated with advanced disease, suggesting that FN1 mRNA expression might serve as a marker for RCC aggressiveness [22]. Although the researchers failed to measure the plasma concentration of FN1, this study supports the results described herein obtained by proteome based screening.

The results of plasma FN1 from 2DICAL analysis were validated in a hundreds-scale cohort using a different methodology. AlphaLISA confirmed that the plasma level of FN1 was up-regulated in the early stage of RCC, which suggested that the FN1 plasma levels might be a tool for screening and diagnosis of RCC. However, there a limitation to introduce FN1 for screening of RCC, because plasma concentrations between patients and controls were overlapped extensively, and FN1 was not examined in benign renal tumors.

RCC comprises five histologically distinct subtypes classified by morphologic and pathologic features including clear cell (75%), papillary (10–15%), chromophobe (5–10%), collecting duct, and unclassified subtypes. We have previously reported that each RCC subtype has a totally different genetic profile by whole genome SNP array [10]. Therefore, each subtype should have a specific biomarker. In this study, we focused on clear cell RCC because it is the most abundant subtype of RCC and hence should be a first target of screening. Our comprehensive study of proteomics led to the possibility that monitoring the level of plasma FN1 could be clinically useful for the screening and diagnosis of RCC patients. The most of the *patients* we analyze were clinical stage I (56 cases / total 77 cases), and they had no symptoms such as febrile and showed normal range of C-reactive protein. Therefore, we believe that FN1 was not derived from acute phase reaction. Reports of the elevation of the plasma level of FN1 in RCC exist in the literature [21], but its clinical usage has not yet been described. One of the reasons may be the lack of applicable clinical test such as ELISA for FN1. The assessment of plasma FN1 levels must be determined for a large scale clinical cohort, but the construction of an easy clinical test such as ELISA will be needed for its completion.

Acknowledgments

We thank Ms. Ayako Igarashi, Ms. Tomoko Umaki, and Ms. Yuka Nakamura for their technical assistance.

Disclosure of potential conflicts of interest

These sponsors had no role in the design of the study, the collection of the data, the analysis and interpretation of the data, the decision to submit the manuscript for publication, or the writing of the manuscript.

Grant supports

Funding was received from the Program for Promotion of Fundamental Studies in Health Sciences conducted by the National Institute of Biomedical Innovation of Japan, and the Third-Term Comprehensive Control Research for Cancer and Research on Biological Markers for New Drug Development conducted by the Ministry of Health, Labour and Welfare of Japan.

Conflicts of interest

None.

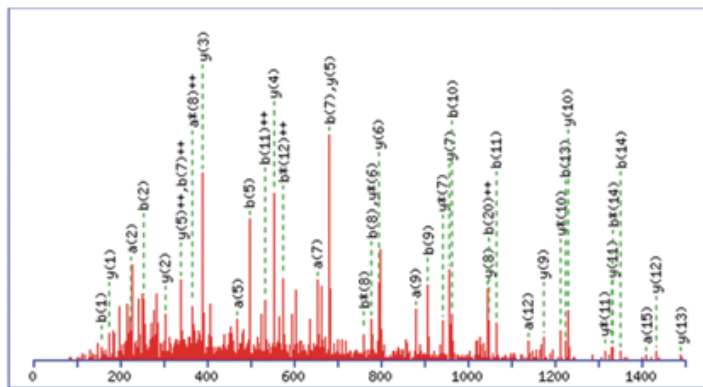
References

- [1] S.H. Landis, T. Murray, S. Bolden, P.A. Wingo. Cancer statistics, 1999, CA Cancer J Clin 49 (1999), 8-31.
- [2] A.J. Schrader, Z. Varga, A. Hegele, S. Pfoertner, P. Olbert, R. Hofmann. Second-line strategies for metastatic renal cell carcinoma: classics and novel approaches, J Cancer Res Clin Oncol 132 (2006), 137-149.
- [3] B.I. Rini, S. Halabi, R. Barrier, K.A. Margolin, D. Avigan, T. Logan et al. Adoptive immunotherapy by allogeneic stem cell transplantation for metastatic renal cell carcinoma: a CALGB intergroup phase II study, Biol Blood Marrow Transplant 12 (2006), 778-785.
- [4] C. Gouttefangeas, A. Stenzl, S. Stevanovic, H.G. Rammensee. Immunotherapy of renal cell carcinoma, Cancer Immunol Immunother 56 (2007), 117-128.
- [5] M. Remzi, M. Marberger. Renal tumor biopsies for evaluation of small renal tumors: why, in whom, and how? Eur Urol 55 (2009), 359-367.
- [6] M. Ono, M. Shitashige, K. Honda, T. Isobe, H. Kuwabara, H. Matsuzuki et al. Label-free quantitative proteomics using large peptide data sets generated by nanoflow liquid chromatography and mass spectrometry, Mol Cell Proteomics 5 (2006), 1338-1347.

- [7] M. Ono, J. Matsubara, K. Honda, T. Sakuma, T. Hashiguchi, H. Nose et al. Prolyl 4-hydroxylation of alpha-fibrinogen: a novel protein modification revealed by plasma proteomics, *J Biol Chem* 284 (2009), 29041-29049.
- [8] A. Negishi, M. Ono, Y. Handa, H. Kato, K. Yamashita, K. Honda et al. Large-scale quantitative clinical proteomics by label-free liquid chromatography and mass spectrometry, *Cancer Sci* 100 (2009), 514-519.
- [9] J. Matsubara, M. Ono, A. Negishi, H. Ueno, T. Okusaka, J. Furuse et al. Identification of a predictive biomarker for hematologic toxicities of gemcitabine, *J Clin Oncol* 27 (2009), 2261-2268.
- [10] A. Yokomizo, K. Yamamoto, K. Furuno, M. Shiota, K. Tatsumi, K. Kuroiwa et al. Histopathologic subtype-specific genomic profiles of renal cell carcinomas identified by high-resolution whole-genome single nucleotide polymorphism array analysis, *Oncol Lett* 1 (2010), 1073-1078.
- [11] TNM Classification of Malignant Tumours. John Wiley and Sons Ltd 2009.
- [12] M. Shitashige, R. Satow, K. Honda, M. Ono, S. Hirohashi, T. Yamada. Regulation of Wnt signaling by the nuclear pore complex, *Gastroenterology* 134 (2008), 1961-1971, 1971 e1961-1964.
- [13] J.D. Storey, R. Tibshirani. Statistical significance for genome-wide studies, *Proc Natl Acad Sci USA* 100 (2003), 9440-9445.
- [14] S.M. Albelda. Role of integrins and other cell adhesion molecules in tumor progression and metastasis, *Lab Invest* 68 (1993), 4-17.
- [15] R.O. Hynes, K.M. Yamada. Fibronectins: multifunctional modular glycoproteins, *J Cell Biol* 95 (1982), 369-377.
- [16] R. Pankov, K.M. Yamada. Fibronectin at a glance, *J Cell Sci* 115 (2002), 3861-3863.
- [17] H. Ro. Fibronectins. Berlin, Heidelberg, New York: Springer.
- [18] W. Brenner, S. Gross, F. Steinbach, S. Horn, R. Hohenfellner, J.W. Thuroff. Differential inhibition of renal cancer cell invasion mediated by fibronectin, collagen IV and laminin, *Cancer Lett* 155 (2000), 199-205.
- [19] J. Lohi, T. Tani, I. Leivo, A. Linnala, L. Kangas, R.E. Burgeson et al. Expression of laminin in renal-cell carcinomas, renal-cell carcinoma cell lines and xenografts in nude mice, *Int J Cancer* 68 (1996), 364-371.
- [20] J. Murata, I. Saiki, J. Yoneda, I. Azuma. Differences in chemotaxis to fibronectin in weakly and highly metastatic tumor cells, *Jpn J Cancer Res* 83 (1992), 1327-1333.
- [21] A. Hegele, A. Heidenreich, J. Kropf, R. von Knobloch, Z. Varga, R. Hofmann et al. Plasma levels of cellular fibronectin in patients with localized and metastatic renal cell carcinoma, *Tumour Biol* 25 (2004), 111-116.
- [22] S. Waalkes, F. Atschekzei, M.W. Kramer, J. Hennenlotter, G. Vetter, J.U. Becker et al. Fibronectin 1 mRNA expression correlates with advanced disease in renal cancer, *BMC Cancer* 10 (2010), 503.

Supplemental material

MS/MS Fragmentation of RPGGEPSPEGTTGQSYNQYSQR
Found in **FINC_HUMAN**, Fibronectin OS=Homo sapiens GN=FN1 PE=1 SV=3
Match to Query 1: 2395.118583 from(799.380137,3+)



Monoisotopic mass of neutral peptide Mr(calc): 2395.0789

Ions Score: 84 **Expect:** 6.3e-008

Matches (Bold Red): 41/252 fragment ions using 78 most intense peaks

#	a	a ⁺⁺	a [*]	a ^{*++}	b	b ⁺⁺	b [*]	b ^{*++}	Seq.	y	y ⁺⁺	y [*]	y ^{*++}	#
1	129.1135	65.0604	112.0869	56.5471	157.1084	79.0578	140.0818	70.5446	R					22
2	226.1662	113.5868	209.1397	105.0735	254.1612	127.5842	237.1346	119.0709	P	2239.985	1120.4962	2222.9585	1111.9829	21
3	283.1877	142.0975	266.1612	133.5842	311.1826	156.0949	294.1561	147.5817	G	2142.9323	1071.9698	2125.9057	1063.4565	20
4	340.2092	170.6082	323.1826	162.0949	368.2041	184.6057	351.1775	176.0924	G	2085.9108	1043.459	2068.8843	1034.9458	19
5	469.2518	235.1295	452.2252	226.6162	497.2467	249.127	480.2201	240.6137	E	2028.8894	1014.9483	2011.8628	1006.435	18
6	566.3045	283.6559	549.278	275.1426	594.2994	297.6534	577.2729	289.1401	P	1899.8468	950.427	1882.8202	941.9137	17
7	653.3365	327.1719	636.31	318.6586	681.3315	341.1694	664.3049	332.6561	S	1802.794	901.9006	1785.7674	893.3874	16
8	750.3893	375.6983	733.3628	367.185	778.3842	389.6958	761.3577	381.1825	P	1715.762	858.3846	1698.7354	849.8713	15
9	879.4319	440.2196	862.4054	431.7063	907.4268	454.217	890.4003	445.7038	E	1618.7092	809.8582	1601.6827	801.345	14
10	936.4534	468.7303	919.4268	460.217	964.4483	482.7278	947.4217	474.2145	G	1489.6666	745.3369	1472.6401	736.8237	13
11	1037.501	519.2542	1020.4745	510.7409	1065.496	533.2516	1048.4694	524.7383	T	1432.6451	716.8262	1415.6186	708.3129	12
12	1138.5487	569.778	1121.5222	561.2647	1166.5436	583.7755	1149.5171	575.2622	T	1331.5975	666.3024	1314.5709	657.7891	11
13	1195.5702	598.2887	1178.5436	589.7755	1223.5651	612.2862	1206.5386	603.7729	G	1230.5498	615.7785	1213.5232	607.2653	10
14	1323.6288	662.318	1306.6022	653.8047	1351.6237	676.3155	1334.5971	667.8022	Q	1173.5283	587.2678	1156.5018	578.7545	9
15	1410.6608	705.834	1393.6342	697.3208	1438.6557	719.8315	1421.6292	711.3182	S	1045.4697	523.2385	1028.4432	514.7252	8
16	1573.7241	787.3657	1556.6976	778.8524	1601.719	801.3632	1584.6925	792.8499	Y	958.4377	479.7225	941.4112	471.2092	7
17	1687.7671	844.3872	1670.7405	835.8739	1715.762	858.3846	1698.7354	849.8713	N	795.3744	398.1908	778.3478	389.6776	6
18	1815.8256	908.4165	1798.7991	899.9032	1843.8205	922.4139	1826.794	913.9006	Q	681.3315	341.1694	664.3049	332.6561	5

Fig. S1. Mascot report of one representative fragment of FN1.

1 MLRGPGPLL LLAVQCLGTA VPSTGASKSK RQAQQMVQPQ SPVAVSQSKP
 51 GCYDNGK**HYQ INQQWERTYL** GNALVCTCYG GSRGFNCESK PEAEETCFDK
 101 YTGNTRYVGD TYERPKDSMI WDCTCIGAGR GRISCTIANR CHEGGQSYKI
 151 GDTWRRPHET GGYMLECVCL GNGKGEWTCK PIAEKCFDHA AGTSYVVGET
 201 WEKPYQGWMM VDCTCLGEGS GRITCTSRNR CNDQDTRTSY RIGDTWSKKD
 251 NRGNLLQCIC TGNGRGEWKC ER**HTSVQTTS SGSGPFTDVR** AAVYQPQPHP
 301 QPPPYGHCVT DSGVVYSVGM QWLKTQGNKQ MLCTCLGNGV SCQETAVTQT
 351 YGGNSNGEPC VLPFTYNGRT FYSCCTTEGRQ DGHLWCSTTS NYEQDQKYSF
 401 CTDHTVLVQT QGGNSNGALC HFPFLYNNHN YTDCSEGRR DNMKWCGBTQ
 451 NYDADQKFGF CPMAAHEEIC TTNEGVMYRI GDQWDKQHDM GHMMRCTCVG
 501 NGRGEWTCIA YSQLRDQCIV DDITYNVNDT FHKRHEEGHM LNCTCFGQGR
 551 GRWKCDPVDQ CQDSETGTFY QIGDSWEKYV HGVRYQCYCY GRGIGEWHCQ
 601 PLQTYPSSSG PVEVFITEP SQPNSHPIQW NAPQPSHISK YILRWRPKNS
 651 VGRWKEATIP GHLNSYTIKG LKPGVVYEGQ LISIQQYGHQ EVTRFDFTTT
 701 STSTPVTANTS VTGETTPFSP LVATSESVTE ITASSFVVS WVSASDTVSGF
 751 RVEYELSEEG DEPQYLDLPS TATSVNIPDL LPGRKYIVNV YQISEDGEQS
 801 LILSTSQT TA PDAPPDPTVD QVDDTSIVVR WSRPQAPITG YRIVYSPSVE
 851 GSSTEINLPE TANSVTLSDL QPGVQYNITI YAVEENQUEST PVVIQQETTG
 901 TPRSDTVPS RDLQFVEVTD VKVTIMWTTP ESAVTGYRVD **VIPVNLPGEH**
 951 **GQRLPISRNT FAEVTGLSPG VTYYFKVFAV** SHGRESKPLT AQQTTKLDAP
 1001 TNLFQFVNEDT STVLRWTTP RAQITGYRLT VGLTRRGQPR QYNVGPSSVK
 1051 YPLRNLIQPAS **EYTDSLVAIK** GNQESPATG VFTTLQPGSS IPPYNTEVTE
 1101 TTIVITWTPA PRIGFKLGVR PSQGGEAPRE VTSDSGSIVV SGLTPGVEYV
 1151 YTIQVLRDGQ ERDAPIVNKV VTPLSPPTNL HLEANPDTGV LTVSWER~~STT~~
 1201 **PDITGYRITT** TPTNGQQGNS LEEVVHADQS SCTFDNLSPG LEYNVSVYTV
 1251 KDDKESVPIS DTIIPAVPPP TDLR**FTNIGP DTMRTWAPP** PSIDLTNFLV
 1301 **RYSPVKNEED** VAELSISPSD NAVVLTNLLP GTEYVVS VYEQHESTPL
 1351 RGRQKTGLDS PTGIDFSDIT ANSFTVHWIA PRATITGYRI RHHPEHFSGR
 1401 PREDRVPHSR NSITLTNLTP GTEYVVSIVA LNGREESPLL **IQQQSTVSDV**
 1451 **PRDLEVVAAT** PTSLLISWDA PAVTVRYYRI TYGETGGNSP VQEFTVPGSK
 1501 STATISGLKP GVDYTITVYA VTGRGDSPAS SKPISINYRT EIDKPSQMQV
 1551 TDVQDNSISV **KWLPSSSPVT GYRVTTTPKN** GPGPTKTKTA GPDQTEMIE
 1601 GLQPTVEYVV SVYAQNPSGE SQPLVQTAVT NIDRPKGLAF TDVDVDSIKI
 1651 AWESPQGQVS RYRVTYSSPE DGIHELPAP DGEEDTAELQ GLRPGSEYTV
 1701 SVVALHDDME SQPLIGTQST AIPAPTDLK TQVTPTLSA QWTPPNVQLT
 1751 GYRVRVTPKE KTGPMEINL APDSSSVVVS GLMVATKYEV SVYALKDTLT
 1801 SRPAQGVVTT LENVSPPRRA RVTDATETTI TISWRKTET ITGFQVDAVP
 1851 ANGQTPIQRT IKPDVRSYTI **TGLQPGTDYK** IYLYTLNDNA RSSPVVIDAS
 1901 TAIDAPSCLR FLATTPNSLL VSWQPPRARI TGYIIKYEP GSPPREVVPR
 1951 PRPGVTEATI TGLEPGTEYT IYVIALKNNQ KSEPLIGRKK TDELPQLVTL
 2001 PHPNLHGPEI LDVPSTVQKT PFVTHPGYDT GNGIQLPGTS GQQPSVGQQM
 2051 IFEEHGFRRT TPPTTATPIR HRPRPYPPNV GEEIQIGHIP REDVDYHLYP
 2101 HGPGLNPNAS TGQEALSQTT ISWAPFQDTS EYIISCHPVG TDEEPLQFRV
 2151 PGTSTSATLT **GLTRGATYNI IVEALKDQQR** HKVREEVVTV GNSVNEGLNQ
 2201 PTDDSCFDPY TVSHYAVGDE WERMSESGFK LLCQCLGFGS GHFRCDSSRW
 2251 CHDNGVNYKI GEKWDRQGEN GQMMSCCLG NGKGEFKCDP HEATCYDDGK
 2301 TYHVGEQWQK EYLGAICST CFGGQRGWRC DNCRRPGGEPE **SPEGTTGQSY**
 2351 **NQYSQRHYQR** TNTNVNCPIE CFMPLDVQAD REDSRE

Matched peptides shown in **Bold Red**

Fig. S2. Peptide hits in the FN1 sequence indicated in red.